POLITECNICO
MILANO 1863

RE.PUBLIC@POLIMI
Research Publications at Politecnico di Milano

**Post-Print**

This is the accepted version of:

L. Bucci, M. Lavagna, D. Guzzetti, K.C. Howell
*Periodic Orbit-Attitude Solutions Along Planar Orbits in a Perturbed Circular Restricted Three-Body Problem for the Earth-Moon System*
Acta Astronautica, Vol. 147, 2018, p. 152-162
doi:10.1016/j.actaastro.2018.03.042

The final publication is available at https://doi.org/10.1016/j.actaastro.2018.03.042

Access to the published version may require subscription.

**When citing this work, cite the original published paper.**

© 2018. This manuscript version is made available under the CC-BY-NC-ND 4.0 license
http://creativecommons.org/licenses/by-nc-nd/4.0/

Permanent link to this version
http://hdl.handle.net/11311/1053188

# PERIODIC ORBIT-ATTITUDE SOLUTIONS ALONG PLANAR ORBITS IN A PERTURBED CIRCULAR RESTRICTED THREE-BODY PROBLEM FOR THE EARTH-MOON SYSTEM

Lorenzo Bucci*, Michèle Lavagna

*Department of Aerospace Science and Technology, Politecnico di Milano, via La Masa 34, 20156, Milano, Italy*

Davide Guzzetti[1], Kathleen C. Howell

*School of Aeronautics and Astronautics, Purdue University, 701 W. Stadium Ave., West Lafayette, IN, 47907-2045, United States*

**Abstract**

Interest on Large Space Structures (LSS), orbiting in strategic and possibly long-term stable locations, is nowadays increasing in the space community. LSS can serve as strategic outpost to support a variety of manned and unmanned mission, or may carry scientific payloads for astronomical observations. The paper focuses on analysing LSS in the Earth-Moon system, exploring dynamical structures that are available within a multi-body gravitational environment. Coupling between attitude and orbital dynamics is investigated, with particular interest on the gravity gradient torque exerted by the two massive attractors. First, natural periodic orbit-attitude solutions are obtained; a LSS that exploits such solutions would benefit of a naturally periodic body rotation synchronous with the orbital motion, easing the effort of the attitude control system to satisfy pointing requirements. Then, the solar radiation pressure is introduced into the fully coupled dynamical model and its effects investigated, discovering novel periodic attitude solu-

*Corresponding author

*Email address:* lorenzo.bucci@polimi.it (Lorenzo Bucci)

[1]Currently at: *School of Aerospace Engineering, Tsinghua University, Qinghuayuan 1, Beijing, 100084, China*

tions. Benefits of periodic behaviours that incorporate solar radiation pressure are discussed, and analysed via the variation of some parameters (e.g reflection/absorption coefficients, position of the centre of pressure). As a final step to refine the current perturbed orbit-attitude model, a structure flexibility is also superimposed to a reference orbit-attitude rigid body motion via a simple, yet effective model. The coupling of structural vibrations and attitude motion is preliminarily explored, and allows identification of possible challenges, that may be faced to position a LSS in a periodic orbit within the Earth-Moon system.

*Keywords:*
Circular Restricted Three-Body Problem, Orbit-Attitude Dynamics, Large Space Structures

---

## 1. Introduction

Nowadays, the Earth-Moon system is attracting more and more interest as a well suited location for near, and far future, long term missions for Large Space Structures (LSS). For designing LSS deep understanding of the orbital and attitude coupled motions is warranted; interesting dynamical structures underlie the orbit-attitude coupled problem, and periodic orbit-attitude solutions may be found. A vehicle which exploits a natural periodic attitude behaviour may allow to relieve some of the control effort from the Attitude Control System (ACS), for example, by satisfying coarse pointing requirements via passive stabilization.

Pioneering studies [1, 2] and more recent research [3, 4] investigate the dynamics of a rigid body at a Lagrangian point; Wong et al. [5] also introduce the coupling between small, linearised orbital motion and attitude dynamics, presenting resonance conditions.

More recent investigations are devoted to the fully coupled orbital-attitude dynamics. Guzzetti and Howell [6, 7, 8] identify orbit-attitude periodic solutions for planar orbits, providing a distinction between elementary planar motions and three-dimensional solutions; Knutson et al. investigate the rigid body motion that is associated with planar [9] and three-dimensional [10, 11] orbits, identifying bounded and unbounded attitude responses. A wide range of techniques to search, identify and exploit coupled orbit-attitude behaviours for space mission design is provided by Guzzetti [12].

Periodic and quasi-periodic orbits, in the Circular Restricted Three-Body Problem (CR3BP), are a valuable tool for mission analysis. A wide range of techniques is currently available for their generation and analysis; several periodic solutions were investigated with numerical techniques [13, 14] and semi-analytical methods [15, 16, 17], both in the three-dimensional and planar case. Recent works [18] provide catalogues for fast generation and analysis of periodic orbits in the Earth-Moon system.

The main scope of the present work is to map the solution space for coupled orbit-attitude dynamics within a perturbed multi-body regime, defining a framework for the operational exploitation of such solutions, and introducing novel tools for their analysis. The study is focused on the Earth-Moon system, although the proposed methods have a general validity for other three-body dynamical systems. A correct utilization of periodic behaviours may, in fact, be an aid to the ACS for a space vehicle that operates in a multi-body gravitational environment, and it may open new scenarios for mission design. Previous works on coupled orbit-attitude dynamics focus on gravity gradient torque only, whereas, at the Lagrangian points of the Earth-Moon system, Solar Radiation Pressure (SRP) torque may be as large as the gravity gradient torque. This work displays that, through a simplified SRP model, periodic orbit-attitude solutions may still exist, when the period of the solution is commensurate to the period of the apparent Sun motion. As an additional step to increase the fidelity of the model, the flexibility of the spacecraft is introduced, analysing its effect on the periodic solutions.

Graphical mapping of the solution space, as introduced in this paper, may be a valuable tool for orbit-attitude dynamics investigation. Numerical targeting strategies provide a method to search periodic orbit-attitude solutions, however, they do not directly enable a clear visualisation of the solution space; a main advantage of graphical mapping techniques is the possibility to intuitively classify families of solutions. A more complete representation of the solution space facilitates comparison between reference and perturbed dynamics. Limitations of graphical mapping are noted, when the number of design variables is increased, since mapping multiple variables into two/three dimensional graphics may be challenging.

The paper is organized as follows: Section 2 provides the models and the nomenclature used for the analysis; Section 3 presents periodic orbit-attitude solutions and their classification into families, leveraging a graphical mapping of the solution space; Section 4 further elaborates the dynamical model, introducing the effect of Solar Radiation Pressure (SRP) and demonstrating

novel periodic solutions, that exploit the SRP torque; Section 5 investigates the effect of structural flexibility on attitude motions obtained under the rigid body approximation, fostering the application of periodic solutions to real space structures; Section 6 provides an applicative example.

## 2. Model and assumptions

### *2.1. Equations of motion*

Let us consider a rigid spacecraft, with an attached principal inertia frame $\hat{x}_b\hat{y}_b\hat{z}_b$, moving under the gravitational pull of two massive attractors $m_1$ and $m_2$, called primaries. The translational dynamics is conveniently described in a rotating frame $\hat{X}_s\hat{Y}_s\hat{Z}_s$, centred in the barycentre of the primaries, whose angular velocity equals the relative mean motion of the two primaries, depicted in Figure 1; $\mathbf{r}_1$ and $\mathbf{r}_2$ represent the position of the spacecraft with respect to the primaries, $r_1$ and $r_2$ denote the norm of $\mathbf{r}_1$ and $\mathbf{r}_2$, respectively. This problem is known as the Circular Restricted Three-Body Problem (CR3BP). Additionally, the $\hat{z}_b$ direction coincides with the $\hat{Z}_s$ axis.

Equations of motion are conveniently normalized with respect to the time, length and mass units of the primary system [14]. Throughout this document, units of measure are omitted when plotting non-dimensional quantities; the absence of units for such quantities is indicated by a dash (-) in the corresponding axis label.

$$\ddot{x} - 2\dot{y} - x = -\frac{1-\mu}{r_1^3}(x+\mu) - \frac{\mu}{r_2^3}(x-1+\mu) \tag{1}$$

$$\ddot{y} + 2\dot{x} - y = -\frac{1-\mu}{r_1^3}y - \frac{\mu}{r_2^3}y \tag{2}$$

The resulting set of equations (1),(2) is governed by a single parameter, called mass ratio, defined as

$$\mu = \frac{m_2}{m_1 + m_2} \tag{3}$$

Although the CR3BP does not possess a closed-form solution, five relative equilibrium points are known. Families of periodic trajectories (in the rotating frame) emanate from the proximity of these equilibria, where the centrifugal and gravitational forces null each other.

Planar rotational dynamics is described by Euler's equation about $\hat{z}_b$ direction.

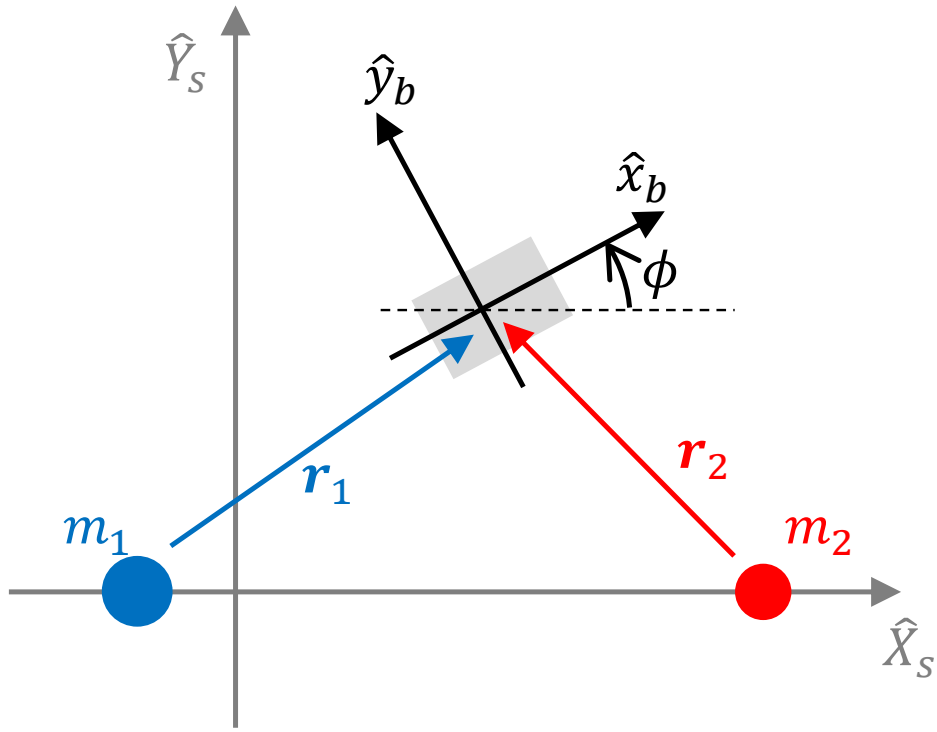


Figure 1: Reference frames

$$\dot{\omega}_z = 3\frac{I_y - I_x}{I_z}\left(\frac{1-\mu}{r_1^3}e_1e_2 + \frac{\mu}{r_2^3}l_1l_2\right) \tag{4}$$

$I_x, I_y$ and $I_z$ in equation (4) denote the principal inertia moments of the spacecraft, about the centre of mass, in the body frame $\hat{x}_b\hat{y}_b\hat{z}_b$; $e_1e_2$ and $l_1l_2$ are the direction cosines of $\mathbf{r}_1$ and $\mathbf{r}_2$, respectively, in body axes $\hat{x}_b\hat{y}_b\hat{z}_b$; the right-hand side denotes the gravity gradient torque [4] exerted by the two primaries.

Observing equation (4), the inertia topology for the spacecraft, in the planar dynamics, may be described through a coefficient $K_z$, defined as

$$K_z = \frac{I_y - I_x}{I_z} \quad , \tag{5}$$

and called inertia ratio.

Considering a planar case only, the rotation of the spacecraft may be represented by a single parameter; the angle $\phi$ is, therefore, selected (referring to Figure 1), being the angle between the $\hat{x}_b$ and the $\hat{X}_s$ axes, measured positively in counterclockwise direction.

### *2.2. Families of orbits*

Within the CR3BP, a large variety of planar periodic motions are accessible, along with a vast literature that discusses numerical techniques to produce those solutions [18, 17, 19]. Figure 2 portrays a sample of planar orbit families that are often proposed as a final destination for lunar exploration, or as a staging location for interplanetary missions. Accordingly, the present analysis focuses on this type of trajectories.

Planar Lyapunov orbits branch out from the collinear Lagrangian points towards the primaries; a few Lyapunov orbits around $L_1$ and $L_2$ are depicted in Figure 2. The $L_2$ orbits might be suitable for trans-lunar infrastructures to support interplanetary travels and lunar activities, while orbits around $L_1$ could be exploited to ease transfers from Earth to lunar orbits and back [20, 21]. Distant Retrograde Orbits (DRO) are particularly appealing for lunar missions design for their high degree of stability [22, 23]; in addition, these orbits encircle both Lagrangian points $L_1$ and $L_2$ and may exploit other orbits transfer manifolds to and from other orbit families [20]; DROs are also among the possible parking orbits considered for NASA's Asteroid Redirect Mission [24]. As common practice in specialized literature, Lyapunov orbits and DROs are classified according to their amplitude $A_y$, measured positively from the $\hat{X}_s$ axis along $\hat{Y}_s$ direction.

## 3. Periodic orbit-attitude solutions

The exploitation of the dynamical coupling between orbit and attitude motion may offer operational possibilities for space mission design. Before including additional external perturbations, the orbit-attitude coupled dynamics for a rigid body are explored with the extension of the gravity action to the attitude motion. Periodic orbit-attitude solutions exist in the planar CR3BP; such solutions are a peculiar combination of translational and angular motion, where the dynamical behaviour repeats at regular intervals both in the trajectory and in the attitude response.

*3.1. Model and algorithm*

To identify periodic orbit-attitude solutions a search method needs to be defined. The search method is developed on the assumption of a rigid spacecraft travelling within an unperturbed CR3BP, where the only forces and torques are induced by the gravitation pull exerted by the two primaries. Kane [25] provides an expression to compute the acceleration induced by a massive point attractor on the centre of mass of an extended rigid body; such expression differs from the well-known gravitational acceleration between two point masses, since a series of terms is added to describe the effect of the finite size of the rigid body. Such additional terms, which depend on the inertia properties of the rigid body, may be negligible with respect to other significant perturbations in the Earth-Moon system [23], and, accordingly, are excluded from the present dynamical model. The set of equations (1) and (2), thus, does not need to be modified.

An algorithm to search for a periodic orbit-attitude solution may be summarized in the following steps:

1. A periodic orbit is obtained, using standard differential correction techniques;
2. The spacecraft topology is defined through a single parameter, $K_z$;
3. The attitude motion is propagated along one orbital period, $T$, for a span of initial body angular velocities, $\omega_z(0)$, between -10 and 10 non-dimensional units, starting with body axes aligned with the rotating frame;
4. For each value $\omega_z(0)$, values of angular velocity $\omega_z(T)$ and rotation angle $\phi(T)$ after one orbit period are collected, and variations with respect to initial conditions $\Delta\omega_z, \Delta\phi$

$$\Delta\omega_z = \omega_z(T) - \omega_z(0) \qquad \Delta\phi = \phi(T) \tag{6}$$

   are computed;[2]
5. A periodic solution is identified when both $\Delta\omega_z$ and $\Delta\phi$ are simultaneously zero (within a tolerance of $10^{-9}$ non-dimensional units, corresponding to $10^{-15}$ rad/s, sufficient for a trade-off between accuracy and computational speed).

[2]Recall that $\phi(0) = 0$, since $\hat{x}_b$ coincides with $\hat{X}_s$ at the initial instant.

A graphical example of the algorithm rationale is depicted in Figure 3 (the term "periodic solution" refers to the value of $\omega_z(0)$ which is necessary, for a given orbit, to establish a periodic planar attitude motion). The identification of the solution, i.e. the point where both the angular velocity residual, $\Delta\omega_z$, and the angle residual, $\Delta\phi$, are zero, is performed as follows, referring to Figure 3:

1. The residuals $\Delta\omega_z$ and $\Delta\phi$ are computed on a small interval of values $\omega_z(0)$, centred on a guessed value, e.g. the solution at the previous step;
2. Two residual curves are constructed, describing angular velocity and angle difference $\Delta\omega_z$ and $\Delta\phi$, respectively, and the residual curve that presents the steepest derivative in the interval, is selected for the next step;
3. The curve with the steepest derivative is interpolated to find an estimate for the value $\omega_z(0)$, where this curve intersects zero. This estimate $\omega_z(0)$ is employed to evaluate the residual function on the remaining curve, also using linear interpolation;
4. If an accurate estimate for the angular velocity $\omega_z(0)$ is identified, the residual functions $\Delta\omega_z$ and $\Delta\phi$ are both zero (within a given tolerance).

The selection of the steepest curve, at point 2, guarantees a good identification of the zero point, better conditioning the interpolation of said curve.

Guzzetti and Howell [7, 8] describe a different algorithm to obtain periodic orbit-attitude solutions, one that leverages a differential correction update for both the spatial orbit and attitude motions to achieve periodicity. The present algorithm fixes the operational orbit and specializes on periodic attitude behaviours strictly associated to a given trajectory.

Furthermore, the algorithm used in the present investigation searches a sole parameter, $\omega_z(0)$, whereas the initial attitude and orbital conditions are kept fixed. It is noted that, as portrayed in Figure 3, the proposed methodology exploits the knowledge of the dynamical behaviour, i.e., searches for a point where both the angle and the angular velocity residuals are zero. Due to the nature of the attitude dynamics problem, the angle and the angular velocity residuals must be zero at the same time, in order for a periodic solution to exist; any other parameter optimization method could be employed to search for $\omega_z(0)$, although losing the advantage of knowing such relation, coming from the dynamical system at hand.

### *3.2. Families of solutions*

Considering a planar periodic orbit, there exist multiple values of $\omega_z(0)$ that guarantee a periodic, planar rotational motion, as noted in [26] during the study of distant retrograde orbits. In general, for the type of solutions currently identified, an initial angular velocity corresponds to $N$ spacecraft rotations, about its $\hat{z}_b$ axis, any one orbit revolution; this observation yields a classification of the solutions into families, each characterized by its own number of rotations, $N$. The sign of $N$ determines the spacecraft rotation direction, which is positive for counterclockwise rotations about the $\hat{z}_b$ axis.

Figure 4 portrays attitude periodic families for DROs, and considering a vehicle with $K_z = 0.8$. The reference periodic trajectory is represented along the horizontal axis, identified by its period; the vertical axis corresponds to the initial angular velocity $\omega_z(0)$, that generates a periodic attitude behaviour, superposed to the reference orbital motion. Throughout this document, different curves correspond to different attitude families.

Observe that the lines belonging to different families, characterized by the number of rotations $N$, may be interpreted as the contour lines of a residual function, which evaluates the residual

$$\Delta(\omega_z(0)) = \Delta\omega_z + \Delta N\phi \tag{7}$$

for a given value of initial angular velocity $\omega_z(0)$, where $\Delta N\phi$ represents the angular residual, $\Delta\phi$, after $N$ rotations. The algorithm in Section 3.1 corresponds, in fact, to a zero-search of the function in equation (7).

A set of sample solutions is depicted in Figure 5, including time histories for the rotation angle and the body angular velocity for a DRO with period of 17 days. In Figure 5, each line renders a different family of attitude periodic solution, as indicated by the number of rotations, $N$. This solution profile matches results obtained by Guzzetti [12].

### *3.3. Attitude periodicity maps*

Once the attitude periodic solutions are identified and classified into families, it is possible to step forward in mapping the solution space. Families of solutions exist for different values of inertia ratio $K_z$, and may be, thus, plotted together to visualize a more informative picture of the solution set.

Recall that, an identification effort for periodic attitude solutions is necessarily tied to the model, and classification, employed. That is, for the current

work, a planar attitude behaviour where the body carries out an integer number, $N$, of rotations per orbit. Other orbit-attitude solutions exist, both in the planar and three-dimensional case [12], and might be also explored and classified.

Attitude periodicity maps represent a useful tool to graphically depict the orbit-attitude solution space. For example, Figure 6 portrays an attitude periodicity map for DROs, considering the whole span of $K_z$ values. The different families may be visually identified, as the lines belonging to the same family are close to each other.

Figures 7 and 8 depict, respectively, attitude periodicity maps for planar Lyapunov orbits around the Lagrangian points $L_1$ and $L_2$. Note that, the $K_z = 0$ case is equivalent to a planar torque-free motion, since such mass distribution would not experience any attitude perturbation due to gravity gradient. Thus, the periodic solutions for $K_z = 0$ correspond to a trivially commensurate orbit-attitude motion, produced by an initial condition $\omega_z(0) = \frac{2\pi N}{T}$, where $T$ is the orbital period. The lines corresponding to $K_z = 0$ are families of hyperbolas. Families associated to no revolutions, $N = 0$, are rendered by straight lines.

A recent work [27] obtained an analytical solution, for planar attitude dynamics of a rigid body located at the Lagrangian points. Such solution might be exploited to obtain the exact value, $\omega_z(0)$, that establishes a periodic attitude behaviour at a Lagrangian point. The exact periodic motion at a collinear Lagrangian point is a good initial guess for Lyapunov orbit periodicity maps. This value guarantees, in fact, a precise initialization of the numerical algorithm that is discussed in Section 3.1.

## 4. Effect of solar radiation pressure

The gravity gradient torque strongly affects the rotational motion for a rigid body, nonetheless, within a multi-body environment, it may not be the largest moment in magnitude. In particular, large space structures with extended surfaces (e.g. solar arrays) are subjected to a large force generated by Solar Radiation Pressure (SRP). SRP forces generally perturb both orbital path and attitude motion; SRP produces, in fact, an acceleration on a vehicle centre of mass, and, also, a torque, when there exists a lever between the solar radiation centre of pressure and the spacecraft centre of mass. Since an additional SRP moment may largely perturb a periodic attitude solution,

that is available within a simplified gravitational model, the inclusion of SRP in the framework is warranted.

Our investigation only explores the effects of SRP on the spacecraft rotational motion; SRP force is not included in the dynamics, thus, the vehicle travels along unperturbed CR3BP reference trajectories. This simplification, in general, is not a sufficiently accurate representation for an actual natural motion, however, a station-keeping system is typically employed to maintain the nominal path in real mission applications. Therefore, the present study may focus on the torque component only, without a loss of generality and applicability of the results.

*4.1. Model for solar radiation pressure*

Consider an infinitesimal surface $dA$, subject to an incoming Sun radiation flux $W_0$ (e.g., $\simeq$1361 $W/m^2$ in the Earth-Moon system). The infinitesimal force generated by SRP [28] may be written as

$$d\mathbf{F}_{SRP} = -\frac{W_0}{c_0} dA(\hat{s}\cdot\hat{n})\left[2C_s|\hat{s}\cdot\hat{n}|\hat{n} + C_d\left(\frac{2}{3}\hat{n}+\hat{s}\right) + C_a\hat{s}\right] \tag{8}$$

depending on the fraction of radiation reflected specularly ($C_s$), diffusively ($C_d$) or absorbed ($C_a$). The symbol $\hat{s}$ denotes the Sun direction, $\hat{n}$ indicates the direction of the normal to the surface $dA$, whereas $c_0$ is the speed of light in vacuum; in the case of an opaque surface, note that the three coefficients $C_s, C_a, C_d$ satisfy the following identity

$$C_s + C_a + C_d = 1 \tag{9}$$

so that only two coefficients are sufficient to fully describe an SRP interaction.

For a preliminary analysis including the SRP torque along orbit-attitude periodic solutions, it is convenient to lump all the external area of the spacecraft into a single flat surface, $A$, whose normal $\hat{n}$ is known in the $\hat{x}_b\hat{y}_b\hat{z}_b$ frame [26]. Such surface is exposed to radiation on both sides, so that the total acceleration acting on the spacecraft may be reduced to a more compact form.

$$\mathbf{a}_{SRP} = -\frac{W_0}{c_0}\frac{A}{m}(\hat{s}\cdot\hat{n})\left[(1-C_s)\hat{s} + \left(2C_s|\hat{s}\cdot\hat{n}| + \frac{2}{3}(1-C_s-C_a)\right)\hat{n}\right] \tag{10}$$

Within a lumped-area approach, the SRP torque may be modelled through the knowledge of the position $\mathbf{d}_c$ of the centre of pressure with respect to the

centre of mass; by assumption, $\mathbf{d}_c$ is fixed in the principal inertia frame. The total torque due to SRP, thus, results in

$$\mathbf{T}_{SRP} = \mathbf{d}_c \times m\mathbf{a}_{SRP} \tag{11}$$

where $m$ is the total mass of the spacecraft, and the SRP acceleration derives from equation (10). In the present planar case, both $\mathbf{d}_c$ and $\mathbf{F}_{SRP}$ lie in the $\hat{X}_s\hat{Y}_s$ plane, so the resulting torque vector is directed as $\hat{Z}_s$.

### *4.2. Sun motion model*

The relative direction of the Sun within the Earth-Moon system may be described, as a first approximation [29], assuming an apparent planar motion within the $\hat{X}_s\hat{Y}_s$ plane, with constant angular velocity, $\Omega_{sun}$. The actual out-of-plane components of the SRP torque are, roughly, 1% of the in-plane component over a synodic period, and may thus be neglected for some orbital periods, within the current framework.

The angle, $\theta_{sun}$, between the Sun and the $\hat{X}_s$ axis is, then, a linear function of time. Figure 9 portrays the Sun position obtained within such a simplified model. Additionally, when the Sun radiation reaches the Earth-Moon system, it is approximated by a parallel ray beam. Since the principal objective is to investigate periodic orbit-attitude solution, the inclusion of SRP generates a periodic excitation, whose period depends on the relationship between the orbital period and that of the apparent Sun motion. If an integer ratio exists between the reference trajectory period and the period of the SRP action, a periodic solution may exist, one whose period is commensurate both to the apparent motion of the Sun, and to the orbit period.

Planar orbits whose period is a submultiple of the apparent Sun period, called Sun-resonant orbits, are a reasonable starting point to explore the interaction of solar radiation with orbit-attitude periodic dynamics. Most of the attention will be devoted to a 1:2 resonance, i.e., the spacecraft carries out two orbital revolutions, while the Sun revolves once in the rotating frame. Such resonance exists both for DROs and Lyapunov orbits.

### *4.3. Modified periodic solutions*

Using Sun-resonant orbits, the search for a periodic attitude solution is extended to an SRP-perturbed environment. If a periodic behaviour is available, that may serve as a mean of passive attitude stabilization for the spacecraft; coupling effects due to gravity gradient and SRP-induced torques

may be cleverly combined to further alleviate the attitude control effort. Virtually, the SRP-induced torque might be not actively compensated; more realistically, ACS will have to control all the perturbations not included in the model, primarily the out-of-plane component of SRP, and those due to the actual motion of the Earth, Moon and Sun.

The algorithm used to search a periodic orbit-attitude solution is analogous to the one presented in Section 3; when SRP torque is introduced, equation (4) is modified using equation (11).

$$\dot{\omega}_z = 3K_z \left( \frac{1-\mu}{r_1^3} e_1 e_2 + \frac{\mu}{r_2^3} l_1 l_2 \right) + \frac{T_{SRP}}{I_z} \tag{12}$$

noting that the torque, $\mathbf{T}_{SRP}$, computed with equation (11), is a scalar in equation (12), since the problem at hand is planar and only the $\hat{Z}_s$ component of the torque vector is necessary to describe rotational dynamics. Some additional parameters define a dynamical response when a SRP torque is included, namely:

- The area-to-mass ratio $A/m$;
- At least two of the coefficients $C_a, C_s, C_d$;
- The position $\mathbf{d}_c$ of the centre of pressure;
- The orientation $\hat{n}$ of the Sun-exposed surface in the principal inertia frame.

Furthermore, the moment of inertia $I_z$ appears directly in equation (12), thus the sole inertia ratio $K_z$ is no longer sufficient. Note also that the initial epoch generally dictates the starting Sun angle $\theta_{sun}(0)$, and, therefore, alters the attitude time history. Mapping the solution space for periodic orbit-attitude behaviours that include SRP, is significantly more complex, because the number of parameters has increased, adding to a large number already in a planar orbit-attitude dynamics. Any combination within the parameter set may be virtually employed; the following discussion considers the initial Sun position $\theta_{sun}(0) = 0$, and the inertia moment $I_z = 96.95 \cdot 10^6$ kgm$^2$, varying the other spacecraft properties, in order to map a portion of the multi-parameter space of solutions.

Consider to practically construct an orbit-attitude periodic solution that includes SRP. Exploiting a 1:2 Sun-resonant DRO ($A_y = 103000$ km), the

correct tuning of the angular velocity $\omega_z(0)$ allows to obtain a periodic attitude behaviour, which synchronizes with the apparent Sun motion. The numerical algorithm follows the scheme described in Section 3.1; the difference lies in the attitude propagation, which is here performed including SRP torque. At this stage, the solution solely including the gravity gradient torque may be employed as initial guess.

The resulting motion is visible in Figure 10. Profiles of angular coordinates are similar, in shape, to those obtained when solely including a gravity gradient perturbation, whereas the periodicity of the solution remains at each two orbital period. For different resonance ratios (e.g. 1:3, 1:4) periodic solutions may be again obtained, with an attitude behaviour that follows the periodicity of the apparent Sun motion.

Beyond assembling an individual periodic response, it is, also, possible to map the solution space, providing a visual tool to identify an angular velocity that yields periodic attitude motion under SRP. Due to a large number of parameters that contribute to SRP, a periodicity map only renders a set of all possible solutions along the reference span of orbits; to preserve an easy visualization of the results, it is convenient to create different maps for different parametric sets.

Figure 11 presents the periodicity map for a LSS in a 1:2 Sun-resonant DRO. The lines correspond again to families of periodic orbit attitude solutions; the horizontal axis represents the arm of the SRP force with respect to the centre of mass for the spacecraft, and it is proportional to the magnitude of the SRP torque. The maps are referred to a structure with external dimensions and mass similar to the International Space Station (ISS); a large area exposed to solar radiation generates a solution very sensitive to SRP torque. Ultimately, if the distance $|\mathbf{d}_c|$ is large enough, the SRP torque is dominant over the gravity gradient moment. Different inertia ratios are presented in the periodicity maps, to analyse the sensitivity of the solutions to such a parameter.

Figure 12 portrays the periodicity map, referred to the same structure, for a 1:2 Sun-resonant Lyapunov orbit around $L_1$ ($A_y = 73500$ km).

Currently available periodicity maps with SRP exhibit a discontinuous behaviour, with gaps and scattered lines, due to an increased numerical difficulty in satisfying tolerances after the introduction of SRP torque. In these cases, the algorithm did not converge with the desired tolerance; such solutions might correspond to bounded behaviours, where a quasi-periodic time history is manifested but attitude periodicity is not guaranteed. Finer mesh

grids and integration tolerance may be employed to overcome such discontinuity, even though numerical precision issues were observed for excessively tight tolerances. Further analysis is warranted to clarify the distinction between bounded and periodic solutions, starting from the investigation of discontinuous regions within the solution space.

The sensitivity to other spacecraft parameter may be explored with the same mapping technique, selecting the desired variable and creating periodicity maps. An additional example of the many possibilities is reported in Figure 13; the set of periodic orbit-attitude solutions on a 1:2 Sun-resonant DRO is mapped, varying the specular reflection coefficient $C_s$ for fixed values of $K_z$ and $C_d$.

## 5. Effect of spacecraft flexibility

This Section addresses the dynamics of a flexible spacecraft in the CR3BP environment, assessing the resulting effect on attitude motion. Large space structures may possess low structural stiffness and poor structural damping, as far as present, and near-future, materials and technologies are employed. Some low frequency natural modes might, then, be excited by the orbital and rotational motion; in return, flexible vibrations may perturb the vehicle nominal trajectory and/or pointing profile. Effects of this perturbation, in general, appear first as an alteration of the attitude dynamics. Accordingly, this work, first explores how the rotational motion for an actual elastic structure may be different from the nominal rigid body solution, for a fixed reference trajectory.

### *5.1. Model*

A lumped-parameters approach is employed to describe the flexible parts of a spacecraft. Because of the discrete representation for flexible components, lumped-parameters models are in general not able to capture the full dynamical spectrum for an elastic structure. They may, however, be suitable to approximate the first fundamental natural modes.

Presented in [26], Figure 14 portrays the model employed for the analysis: a rigid spacecraft, with inertia moment $\bar{I}_z$, with $N_f$ flexible components attached. Each $i$-th flexible part is modelled as a Single-Degree-Of-Freedom (SDOF) system, with mass $\bar{m}_i$, stiffness $\bar{k}_i$, connected to the rigid body at the coordinates $\bar{x}_i, \bar{y}_i$. The variable $\bar{s}_i$ indicates the elongation for the corresponding spring, and may represent a generic quantity that is associated

with a flexible behaviour. The angle $\bar{\alpha}_i$ describes the orientation for the $i$-th SDOF system; for the present investigation, orientation angles, $\bar{\alpha}_i$, are fixed. Let us also denote, with $\bar{\Omega}_i = \sqrt{\bar{k}_i/\bar{m}_i}$, the fundamental frequency of each flexible part. The rotational and vibrational motion are constrained within the $\hat{x}_b\hat{y}_b$ plane, which coincides with the $\hat{X}_s\hat{Y}_s$ plane for the present planar dynamical framework.

*5.2. Equations of motion*

Employing a Lagrangian approach [23, 30], $N_f + 1$ coupled equations of motion are obtained: that is, a set of $N_f$ equations that describe flexible dynamics, plus one equation for rotational dynamics as a first approximation. No external forces are assumed to act on the masses $\bar{m}_i$. Gravitational pull of the Earth and the Moon is only applied to the rigid part of the spacecraft, therefore, with no effect on structural dynamics.

Each SDOF system is governed by a second-order differential equation

$$\bar{m}_i\ddot{\bar{s}}_i + (\bar{k}_i - \bar{m}_i\omega_z^2)\bar{s}_i = \bar{m}_i\omega_z^2 L_i - \bar{m}_i\dot{\omega}_z A_i \tag{13}$$

where two auxiliary coefficients have been defined

$$L_i = (\bar{x}_i \cos\bar{\alpha}_i + \bar{y}_i \sin\bar{\alpha}_i) \tag{14}$$

$$A_i = (\bar{x}_i \sin\bar{\alpha}_i - \bar{y}_i \cos\bar{\alpha}_i) \tag{15}$$

for a more compact notation. The following equation governs rotational dynamics

$$\dot{\omega}_z \left[ \bar{I}_z + \sum_{i=1}^{N_f} \bar{m}_i(\bar{s}_i^2 + \bar{x}_i^2 + \bar{y}_i^2 + 2\bar{s}_i L_i) \right] + \omega_z \sum_{i=1}^{N_f} 2\bar{m}_i(\bar{s}_i\dot{\bar{s}}_i + \dot{\bar{s}}_i L_i) = T_z - \sum_{i=1}^{N_f} \bar{m}_i\ddot{\bar{s}}_i A_i \tag{16}$$

where $T_z$ represents the sum of all external torques acting on the spacecraft (e.g., gravity gradient, SRP torque, etc.).

It is interesting to analyse how the attitude dynamics is affected by structural vibrations; looking at equation (16), one may observe the followings:

- The first term (between square brackets) represents the overall inertia moment, $I_z$, of the body, considering both the rigid and the flexible sections;

- The second term is a non-linear coupling term, between the body angular velocity and linear velocities of the flexible parts;
- The last expression is an equivalent torque, exerted on the spacecraft, due to the inertia forces of the vibrating parts.

*5.3. Case study: high structural frequencies*

The following paragraphs provide a deeper analysis of the flexible dynamics, developing the formulation under some working assumptions. It is usually reasonable to assume, for present and near-future space structures, that

$$\bar{\Omega}_i \gg \omega_z, \frac{2\pi}{T} \qquad \forall\ i \tag{17}$$

i.e., the orbital and attitude natural frequencies are much lower than the structural ones. Under such assumption, the behaviour of a spacecraft is dominated by the rigid body motion, and the flexible contributions in the left-hand term of equation (16) may be dropped, since they are first- or second-order infinitesimal quantities [26, 23]. Equation (13) may be further reduced to

$$\ddot{\bar{s}}_i + \bar{\Omega}_i^2 \bar{s}_i = \omega_z^2 L_i - \dot{\omega}_z A_i \tag{18}$$

neglecting the gyroscopic contribution to stiffness. It is further assumed that, small flexible vibrations do not significantly perturb an attitude motion, and, thus, the time history for the spin rate $\omega_z$ may be obtained by integrating the rigid body motion, along a fixed orbit, with gravity gradient torque (SRP may be added, too). Having the angular velocity, $\omega_z$, a periodic behaviour, equation (18) describes a SDOF, periodically forced system. The resulting problem may be investigated as follows:

1. A rigid body, periodic orbit-attitude solution is obtained, with the techniques described in the previous sections;
2. The time history for the angular velocity, $\omega_z$, associated to the rigid body solution (with gravity gradient solely, or GG+SRP), is acquired;
3. The set of $N_f$ equations (18) are solved numerically, or in closed form if the solution for the variable $\omega_z$ is approximated with an analytic expansion (e.g. Fourier series);
4. The resulting values $\ddot{\bar{s}}_i$ are employed to compute the attitude perturbation due to vehicle flexibility.

The attitude perturbation that results from point 4 of the list above is the right-hand term of equation (16), which may be integrated, again, including both external torques and such perturbation. When equation (17) is a valid model, the flexibility of the spacecraft does not significantly perturb the attitude motion, resulting in a small, periodic torque with no secular component (as a first approximation in the present framework).

However, a potential value within this analysis is the computation of the coordinates $\bar{s}_i$, which may be employed to foresee maximum and mean displacements, and provide preliminary information for structural analysis.

### *5.4. Case study: low structural frequencies*

Complementary to the analysis for high frequencies, is the case when structural frequencies are very low, in the neighbourhood of the attitude and orbital frequencies, since strong coupling may arise between rotational motion, orbital path and vibrations of flexible components. The analysis for low structural frequencies is, at present, less connected to a real application, acknowledging the fact that disposing a highly flexible structure in space is beyond the current technological capability; nonetheless, it is included for completeness, and to provide a preliminary insight into the problem. The sole attitude dynamics is considered, in analogy with the previous Section; the orbital motion may be investigated in future studies.

Dropping the assumption reported in equation (17), the attitude motion needs to be numerically integrated, together with the motion for the flexible parts. In fact, a non-linear coupling between the elastic displacements and the body angular velocity, i.e., the second term in equation (16), arises, and may be significant in the description of the fully-coupled motion.

Figure 15 portrays the angular velocity time history for a spacecraft with lowered structural frequencies; the perturbed attitude profile is displayed together with the nominal solution, that is obtained using a rigid body periodic orbit-attitude solution. The reference orbit is a DRO with period $T = 14.75$ days, which corresponds to a frequency of $7.85 \times 10^{-7}$ Hz.

As the relative time scaling among the fundamental frequencies for the coupled motion (orbit, attitude, and flexible behaviours) varies, different responses are observed:

- When structural angular frequencies are low with respect to the orbit-attitude motion ones (Figure 15a), the attitude motion encounters

small short-period perturbations, which do not hinder the overall behaviour; the flexibility of the spacecraft may, thus, be considered as a perturbation of the rigid body attitude solution.

- If structural frequencies are in the neighbourhood of the orbital frequency, a strong coupling arises between attitude motion and elastic vibrations. The angular velocity time history (Figure 15b) reveals a strongly non-linear behaviour; its periodicity is no longer dominated by the rigid body solution, since large oscillations are due to a flexible structure excitation.

- When structural frequencies are much lower than those of orbital and attitude motion, the elastic components dictate the overall spacecraft behaviour. The body angular velocity (Figure 15c) rapidly deviates from the nominal behaviour, settling in the neighbourhood of zero; accordingly, the movement of the flexible parts is dominant, as their inertia forces attenuate the impact of the gravity gradient torque on the final response.

These observations may be employed for preliminary spacecraft design, to assess the effect of flexible components (e.g. large solar arrays, deployable modules, etc.) on the attitude motion. If the assumption in equation (17) is accurate, the spacecraft dynamics analysis may be based on the rigid body solutions, and flexible behaviours may be treated as small attitude perturbations.

## 6. 1:2 Sun resonance DRO example: full dynamical model

A final applicative example is provided, in order to highlight the operational possibilities opened by a correct exploitation of the natural environment. A 1:2 Sun resonant DRO ($A_y$ = 103000 km, $T$ = 15 days) is envisaged as promising staging location for a LSS in lunar vicinity, since the orbit period resonance with the Sun period allows to identify periodic orbit-attitude solutions which include the effect of SRP; furthermore, the stability properties of the DRO family provide a high degree of robustness towards perturbations. A sample LSS is employed for the analysis, with a specular reflection coefficient $C_s = 0.4$, absorption coefficient $C_a = 0.6$, moment of inertia $I_z = 96.95 \cdot 10^6$ kgm$^2$, area-to-mass ratio $A/m = 0.016$ m$^2$/kg, and three flexible modes, with principal frequencies of $10^{-6}, 10^{-5}, 10^{-4}$ Hz. Considering

a nominal solution, obtained with the techniques and models (CR3BP + GG + SRP + flexibility) presented throughout the paper, Figure 16 portrays the deviations, with respect to such nominal solution, of the rotation angle and angular velocities time history. A perturbation on the initial angular velocity equal to the 1% of the nominal value is considered, together with a 5 degrees error in the initial angle; furthermore, a 1% modelling error is introduced in the parameters $I_z, C_a, C_s, A/m$. It is noted that the resulting deviation from the nominal profile is small, and bounded in amplitude; the non-divergence of the perturbed solution is a preliminary demonstration that some periodic orbit-attitude behaviours, within simpler dynamical models, may serve as stable and robust references for mission design in higher fidelity. Further studies are, however, required to explore the effects of additional perturbations, that are not incorporated into the current dynamical model.

## 7. Final remarks

The paper presents a framework to investigate planar orbit-attitude dynamics in both a standard, and a perturbed CR3BP environment.

Periodic solutions, where both orbital and rotational motion are repeated regularly, may be established, assuming the spacecraft to be a rigid body perturbed by gravity gradient torque only. Such solutions are systematically classified into families, and periodicity maps are employed to more efficiently visualize the solution space. These maps may provide the mission analyst a valuable tool for a preliminary analysis, allowing to recognize desired or undesired attitude behaviours without using extensive numerical simulations within complex, higher-fidelity models. The periodic orbit-attitude solutions might offer novel possibilities for future missions involving large space structures, and the results of the paper may serve as a starting point for further investigations.

The model is, then, refined with the introduction of Solar Radiation Pressure (SRP) torque, combined with a simplified representation of the spacecraft. Artificially fixing the reference orbit, periodic orbit-attitude solutions may still be possible, in condition of resonance with the Sun apparent motion in the rotating frame.

Future studies may include the investigation of SRP perturbation on the trajectory, exploring its consequences when both, nominally periodic, orbit and attitude motions are simultaneously perturbed. Novel periodic orbit-

attitude solutions may be searched for and explored in such a refined model, exploiting the results obtained within the presented assumptions.

Eventually, the perturbation induced on the attitude motion by flexible components is introduced. Such perturbation remains small and bounded as long as the natural frequencies of the flexible structure are much higher than those representative of the orbital attitude motion; when the two sets of natural frequencies possess the same order of magnitude, strong non-linear couplings may emerge, leading to possible diverging behaviour. The results are obtained with a lumped-parameters first order model; more refined models can offer a greater insight on the structural-attitude coupling, and further analyses might highlight peculiar behaviours in case or structures with large compliance.

## References


[1] T. R. Kane, E. L. Marsh, Attitude stability of a symmetric satellite at the equilibrium points in the restricted three-body problem, Celestial Mechanics 4 (1) (1971) 78–90.

[2] W. J. Robinson, Attitude stability of a rigid body placed at an equilibrium point in the restricted problem of three bodies, Celestial Mechanics and Dynamical Astronomy 10 (1) (1974) 17–33.

[3] A. Abad, M. Arribas, A. Elipe, On the attitude of a spacecraft near a lagrangian point, Bulletin of the Astronomical Institutes of Czechoslovakia 40 (1989) 302–307.

[4] E. Brucker, P. Gurfil, Analysis of gravity-gradient-perturbed rotational dynamics at the collinear lagrange points, The Journal of the Astronautical Sciences 55 (3) (2007) 271–291.

[5] B. Wong, R. Patil, A. Misra, Attitude dynamics of rigid bodies in the vicinity of the lagrangian points, Journal of Guidance, Control, and Dynamics 31 (1) (2008) 252–256.

[6] D. Guzzetti, K. C. Howell, Coupled orbit-attitude dynamics in the three-body problem: a family of orbit-attitude periodic solutions, in: AIAA/AAS Astrodynamics Specialist Conference, 2014.

[7] D. Guzzetti, K. C. Howell, Natural periodic orbit-attitude behaviors for rigid bodies in three-body periodic orbits, in: 66th International Astronautical Congress (IAC), 2015.

[8] D. Guzzetti, K. C. Howell, Natural periodic orbit-attitude behaviors for rigid bodies in three-body periodic orbits, Acta Astronautica 130 (2017) 97–113.

[9] A. J. Knutson, D. Guzzetti, K. C. Howell, M. Lavagna, Attitude responses in coupled orbit-attitude dynamical model in Earth–Moon lyapunov orbits, Journal of Guidance, Control, and Dynamics 37 (7) (2015) 1264–1273.

[10] A. J. Knutson, Application of kane's method to incorporate attitude dynamics into the circular restricted three-body problem, Ph.D. thesis, Purdue University (2012).

[11] A. J. Knutson, K. C. Howell, Coupled orbit and attitude dynamics for spacecraft comprised of multiple bodies in Earth-Moon halo orbits, in: 63rd International Astronautical Congress (IAC), 2012.

[12] D. Guzzetti, Coupled orbit-attitude mission design in the circular restricted three-body problem, Ph.D. thesis, Purdue University (May 2016).

[13] M. Hénon, Numerical exploration of the restricted problem, Astronomy and Astrophysics 1 (1969) 223–238.

[14] V. Szebehely, Theory of Orbits: The Restricted Problem of Three Bodies, Academic Press, New York, 1967.

[15] J. V. Breakwell, J. V. Brown, The halo family of 3-dimensional periodic orbits in the Earth–Moon restricted three-body problem, Celestial Mechanics 20 (4) (1979) 389–404.

[16] D. L. Richardson, Analytic construction of periodic orbits about the collinear points, Celestial Mechanics 22 (3) (1980) 241–253.

[17] G. Gómez, J. Llibre, R. Martínez, C. Simó, Dynamics and Mission Design Near Libration Points. Fundamentals: The Case of Collinear Libration Points, Vol. 1, World Scientific, 2001.

[18] D. C. Folta, N. Bosanac, D. Guzzetti, K. C. Howell, An Earth–Moon system trajectory design reference catalog, Acta Astronautica 110 (2015) 341–353.

[19] G. Gómez, A. Jorba, J. Masdemont, C. Simó, Dynamics and Mission Design Near Libration Points. Advanced methods for Collinear Points, Vol. 3, World Scientific, 2001.

[20] L. Capdevila, D. Guzzetti, K. C. Howell, Various transfer options from earth into distant retrograde orbits in the vicinity of the moon, in: AAS/AIAA Space Flight Mechanics Meeting, 2014.

[21] M. Vaquero, K. C. Howell, Leveraging resonant-orbit manifolds to design transfers between libration-point orbits, Journal of Guidance, Control, and Dynamics 37 (4) (2014) 1143–1157.

[22] O. C. Winter, The stability evolution of a family of simply periodic lunar orbits, Planetary and Space Science 48 (1) (2000) 23–28.

[23] L. Bucci, Coupled orbital-attitude dynamics of large structures in non-keplerian orbits, Master's thesis, Politecnico di Milano (April 2016).

[24] Asteroid redirect robotic mission (arrm) reference mission concept study public information package v1 (NASA, 2013).

[25] T. R. Kane, P. W. Likins, D. A. Levinson, Spacecraft Dynamics, McGraw-Hill, New York, 1983.

[26] L. Bucci, M. Lavagna, Coupled dynamics of large space structures in lagrangian points, in: 6th International Conference on Astrodynamics Tools and Techniques, 2016.

[27] L. Bucci, M. Lavagna, Nonlinear attitude dynamics of a rigid body at the lagrangian points, in: 27th AAS/AIAA Spaceflight Mechanics Meeting, 2017.

[28] J. R. Wertz, Spacecraft Attitude Determination and Control, Kluwer Academic Publishers, Dordrecht, 1990.

[29] W. S. Koon, M. W. Lo, J. E. Marsden, S. D. Ross, Dynamical Systems, the Three-Body Problem and Space Mission Design, Springer-Verlag, New York, 2007.

[30] D. Guzzetti, Large space structures dynamics in a multi-body gravitational environment, Master's thesis, Politecnico di Milano (July 2012).

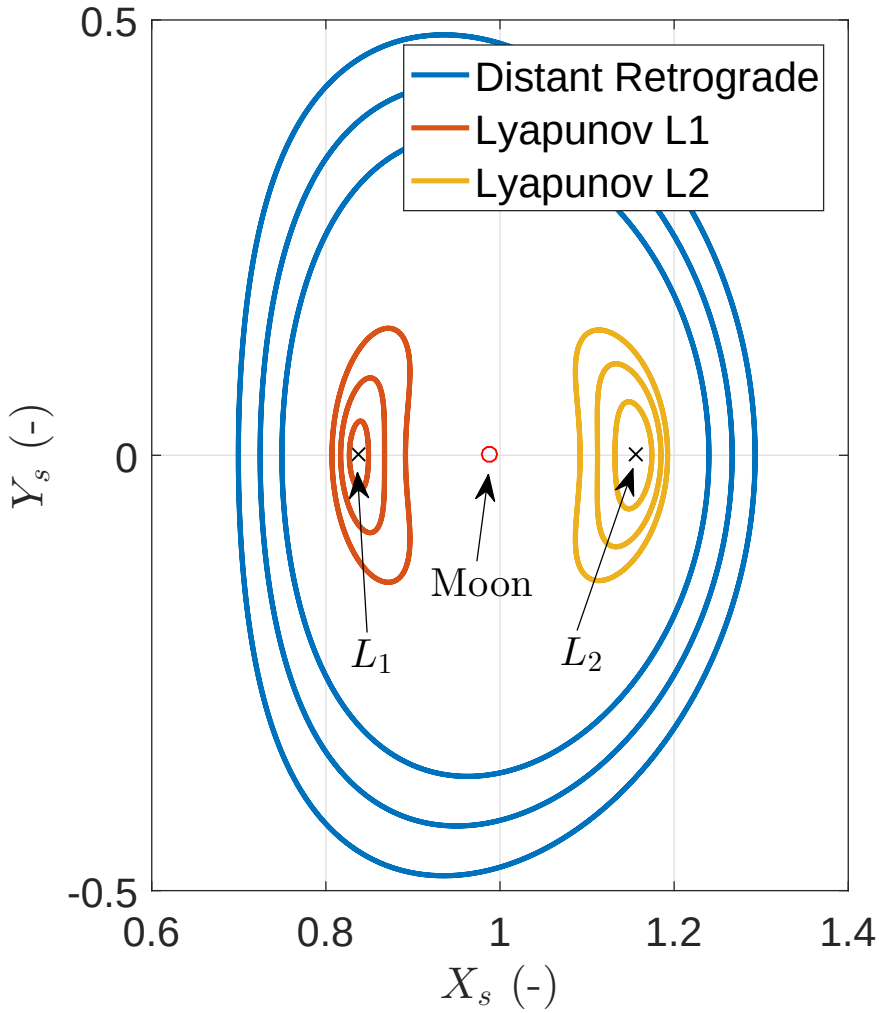


Figure 2: Planar CR3BP orbit families

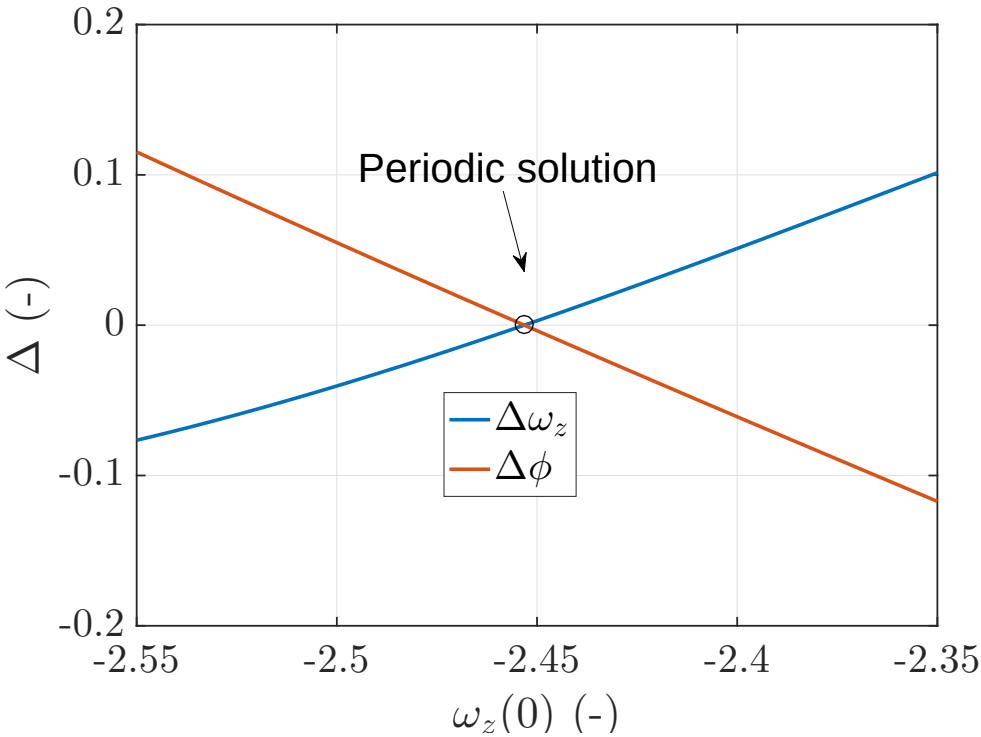


Figure 3: Angle and angular velocity residuals, to identify the periodic solution

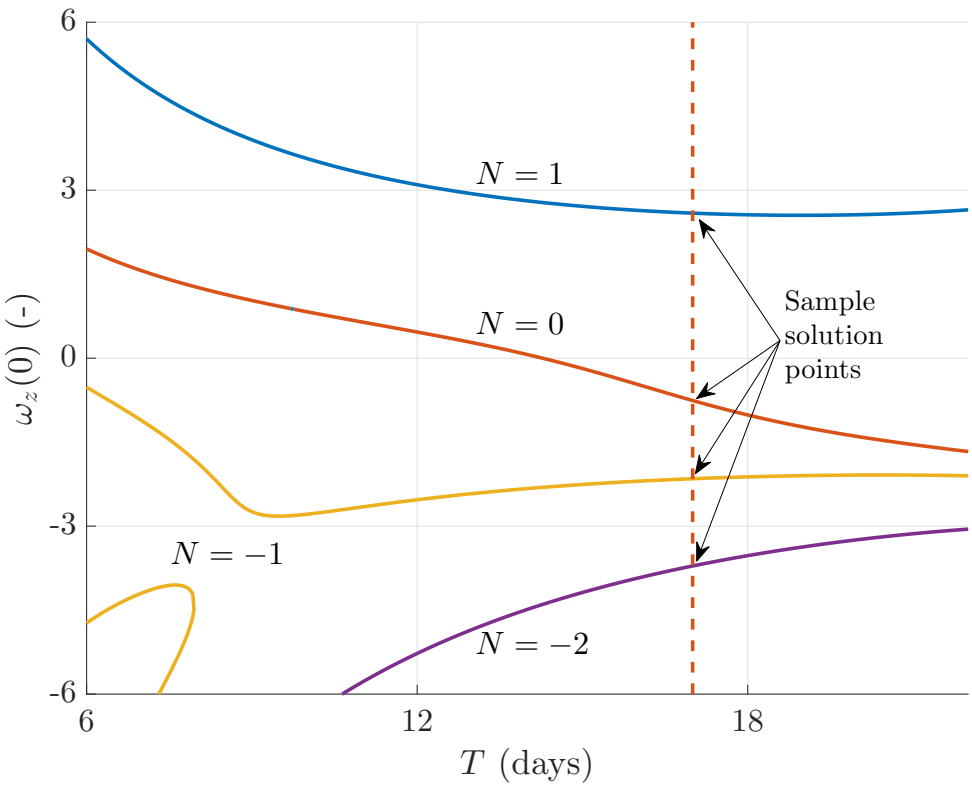


Figure 4: Solution families for DROs, $K_z = 0.8$

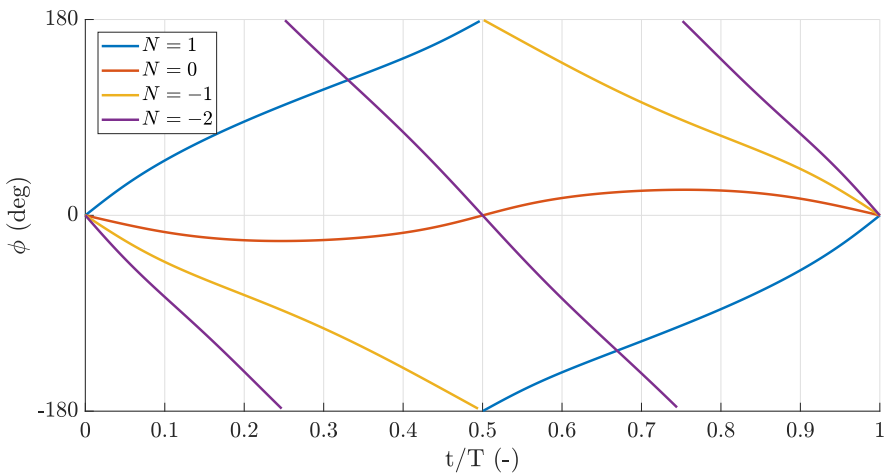


(a) Rotation angle

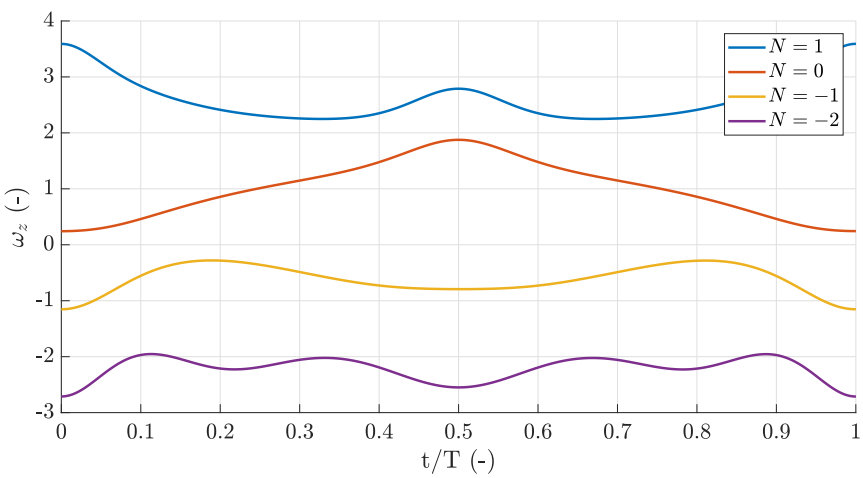


(b) Angular velocity

Figure 5: Sample periodic solution $K_z = 0.8$, DRO with $T = 17$ days

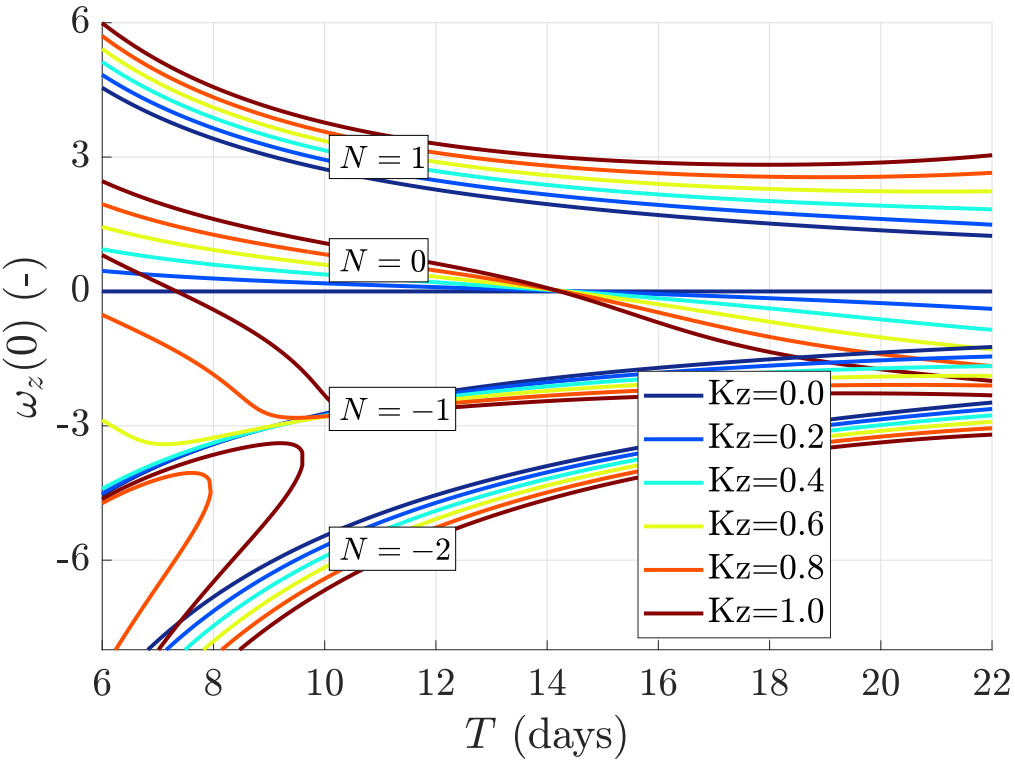


Figure 6: Periodicity maps for distant retrograde orbits. $A_y = 36300 - 228100$ km

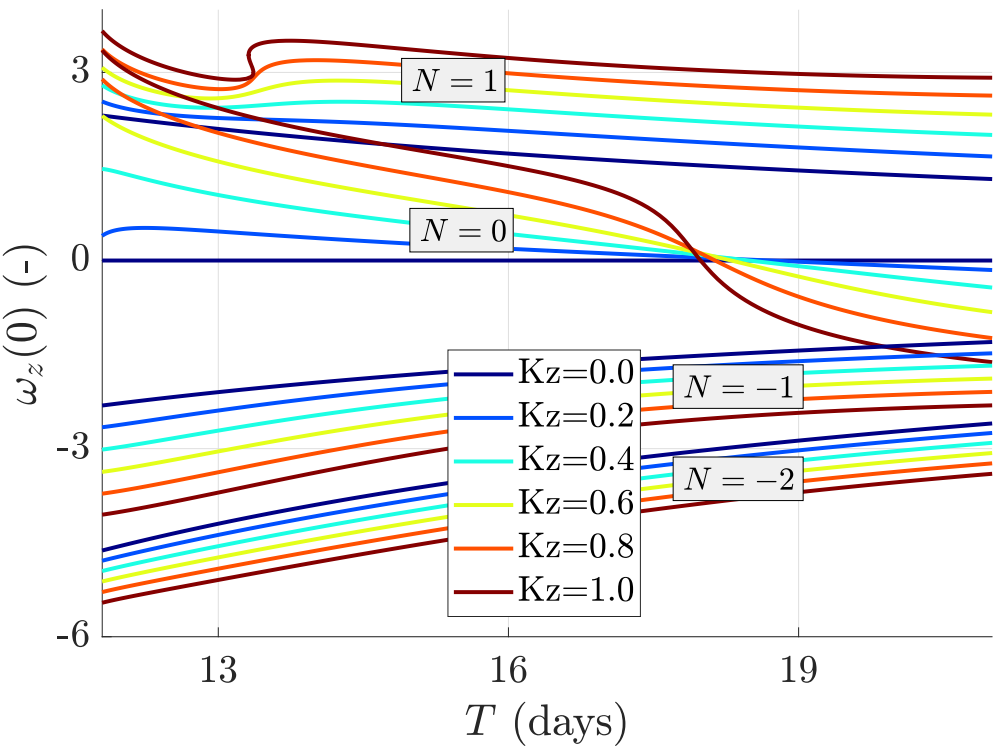


Figure 7: Periodicity maps for $L_1$ Lyapunov orbits. $A_y = 1200 - 183800$ km

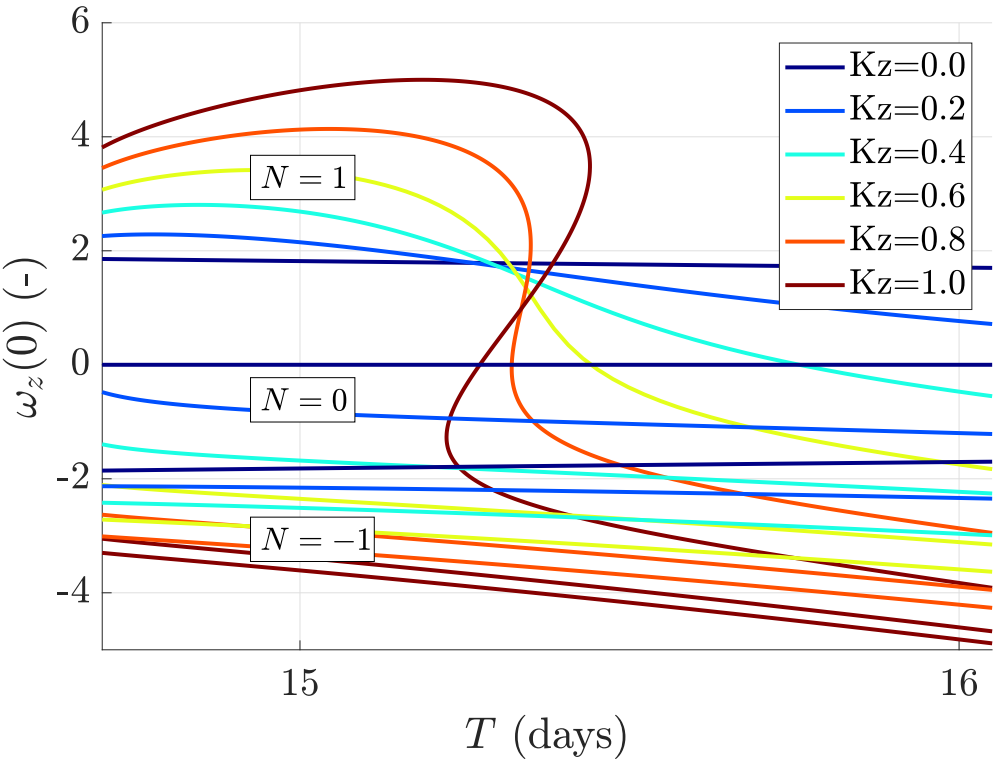


Figure 8: Periodicity maps for $L_2$ Lyapunov orbits (note the partial overlapping of families $N = 0$ and $N = -1$). $A_y = 6000 - 76000$ km

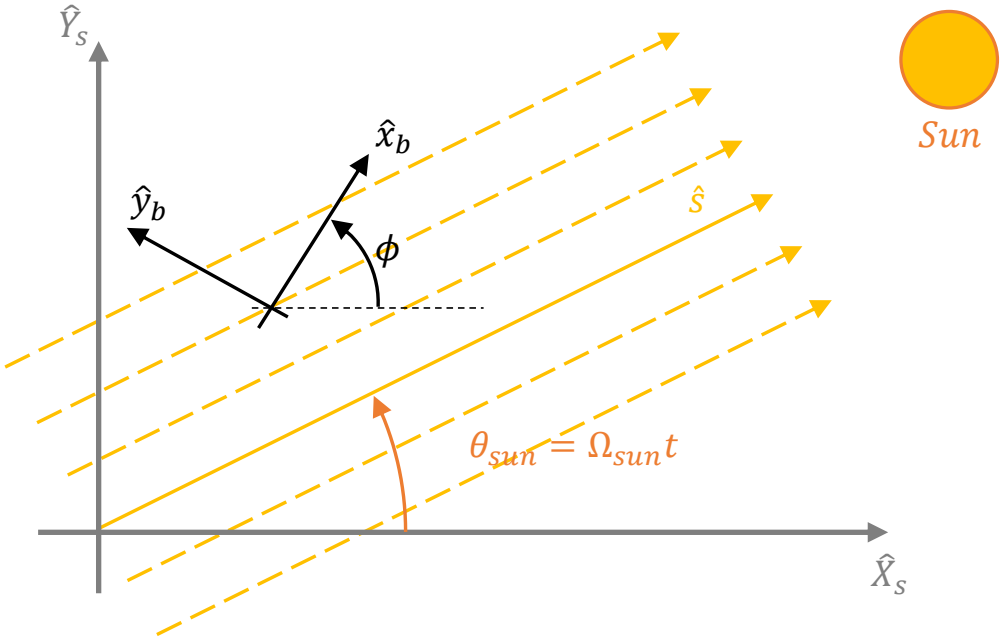


Figure 9: Apparent Sun motion in the CR3BP

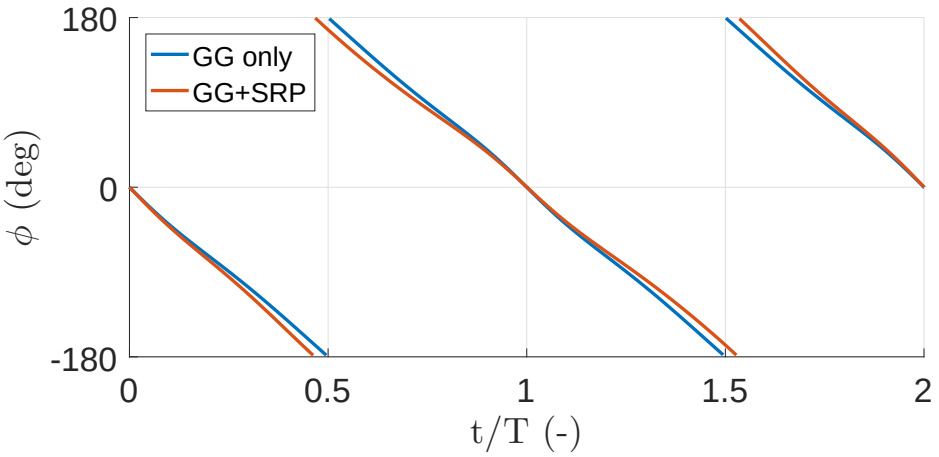


(a) Rotation angle

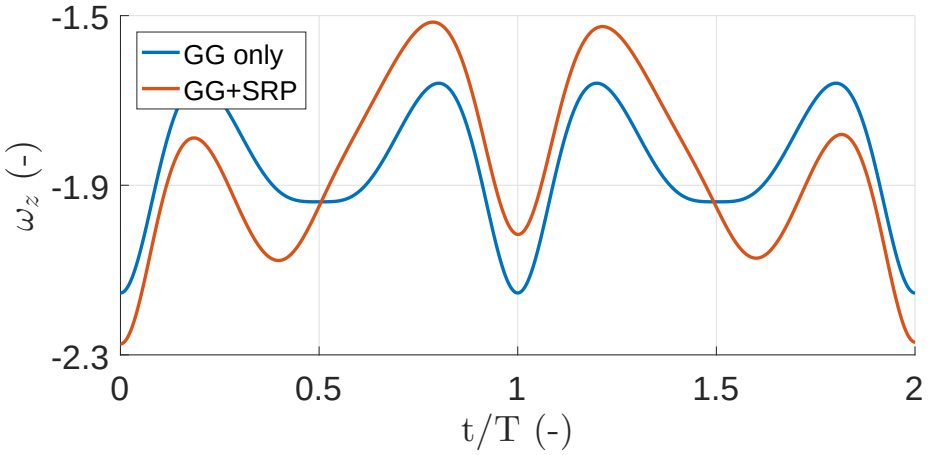


(b) Angular velocity

Figure 10: Sample solution with SRP, $K_z$=0.6, $C_s$=0.4, $C_a$=0.6, $A/m$=0.016 m$^2$/kg, 1:2 Sun resonant DRO, $|\mathbf{d}_c|$=7.5 mm

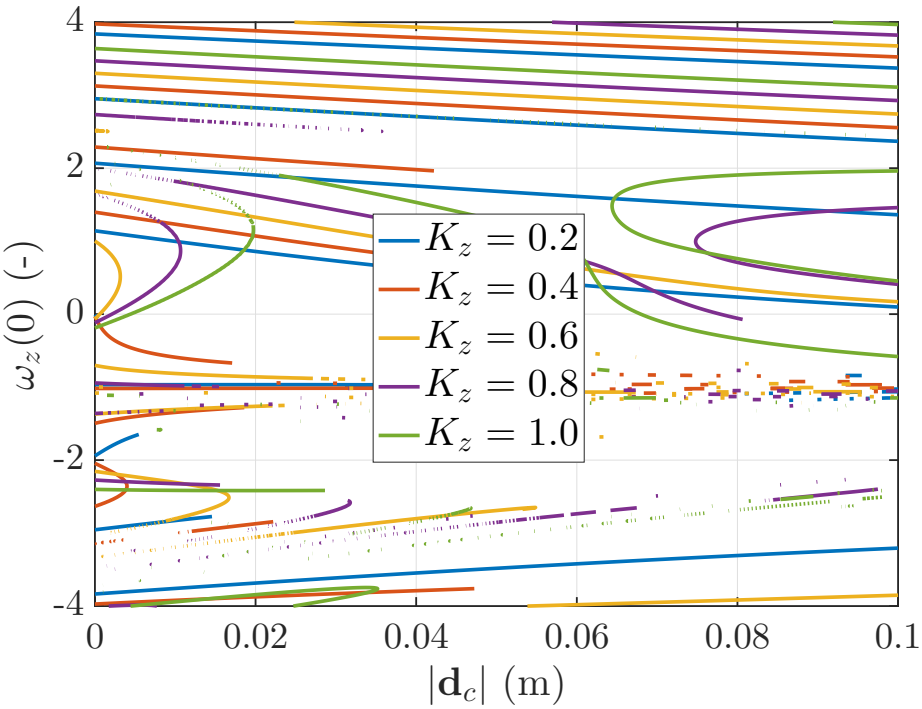


Figure 11: Periodicity map with SRP, $C_s$=0.4, $C_a$=0.5, $A/m$=0.016 m$^2$/kg, 1:2 Sun resonant DRO

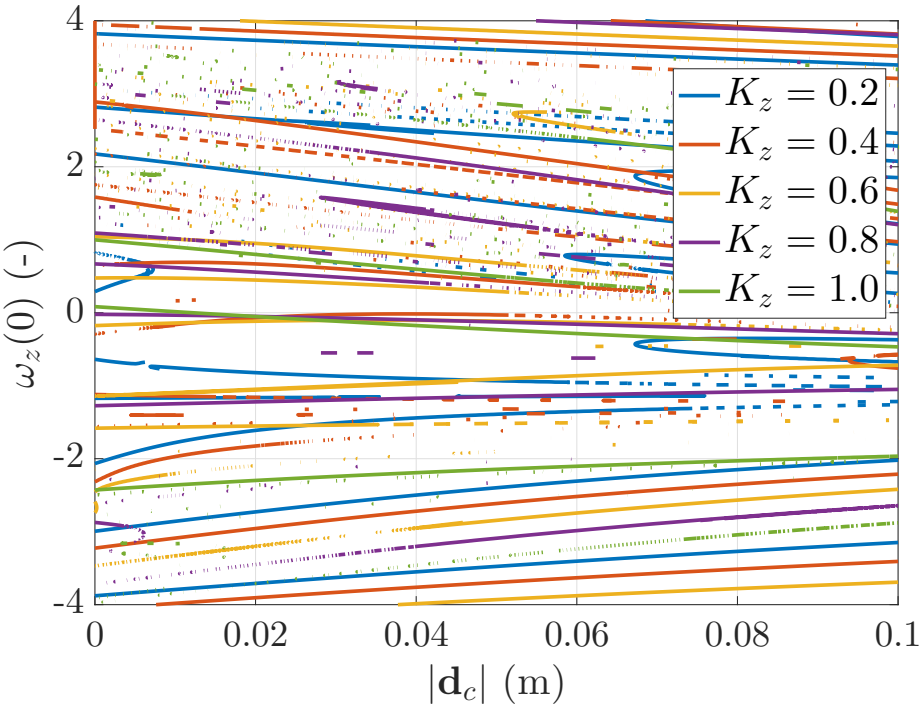


Figure 12: Periodicity map with SRP, $C_s$=0.4, $C_a$=0.5, $A/m$=0.016 m$^2$/kg, 1:2 Sun resonant $L_1$ Lyapunov orbit

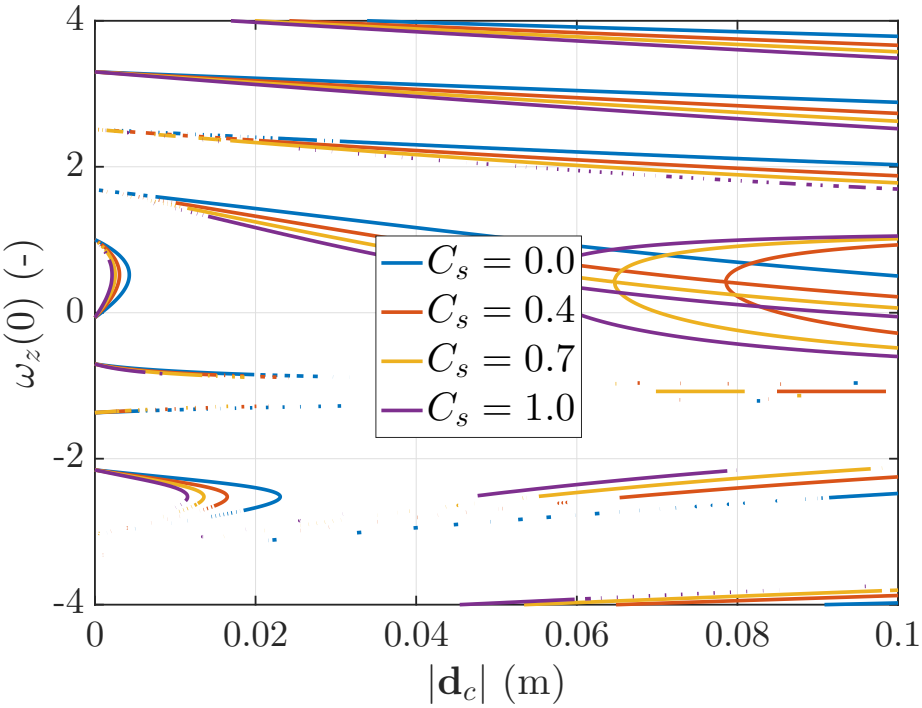


Figure 13: Periodicity map with SRP, $K_z$=0.6, $C_d$=0, $A/m$=0.016 m$^2$/kg, 1:2 Sun resonant DRO

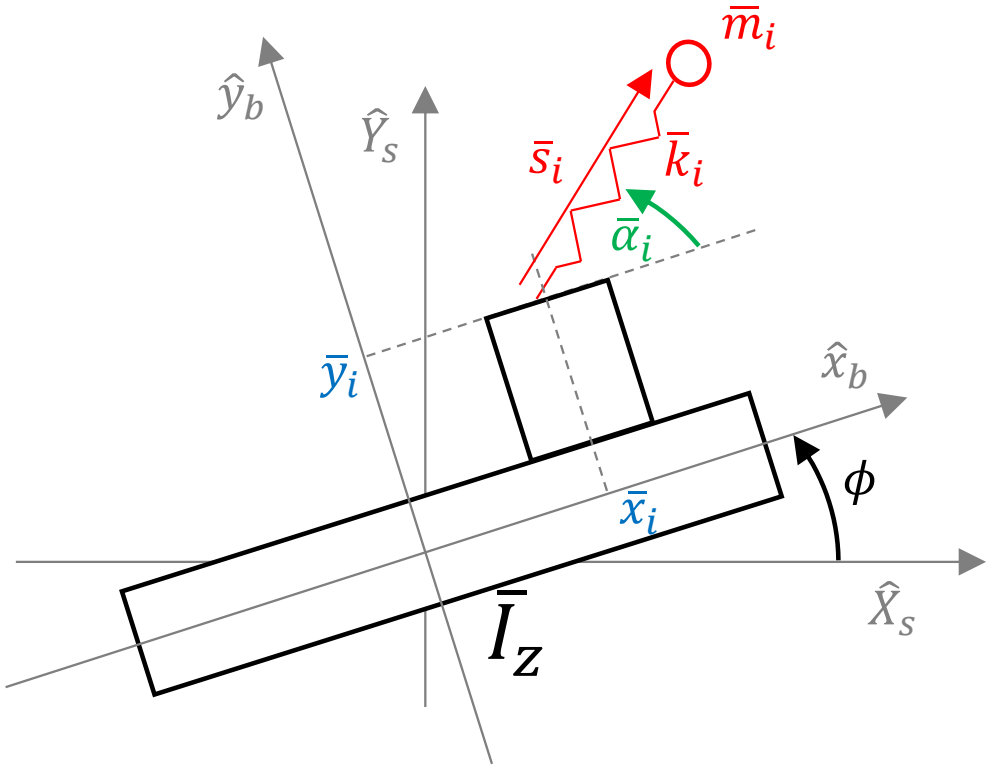


Figure 14: Spacecraft lumped-parameters model

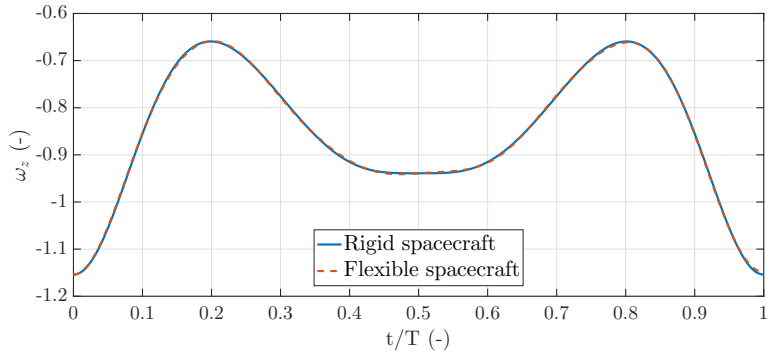


(a) Natural frequencies $\mathcal{O}(10^{-6})$ Hz

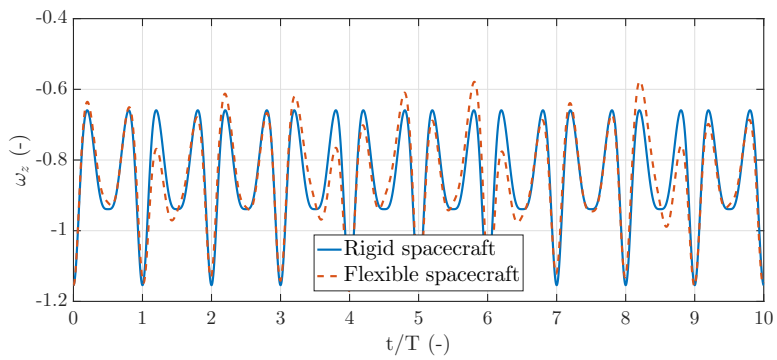


(b) Natural frequencies $\mathcal{O}(10^{-7})$ Hz

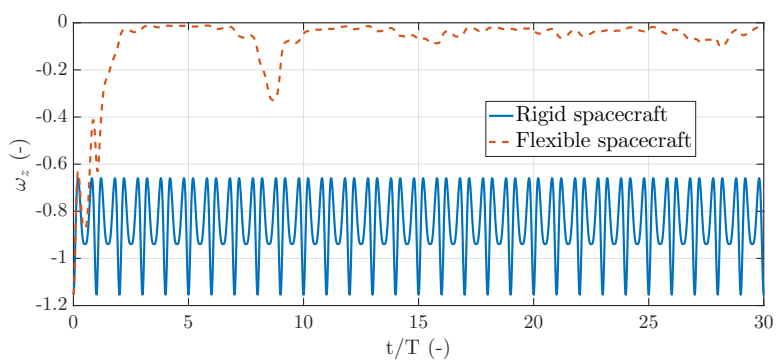


(c) Natural frequencies $\mathcal{O}(10^{-8})$ Hz

Figure 15: Body angular velocity with low structural frequencies $\bar{\Omega}_i$

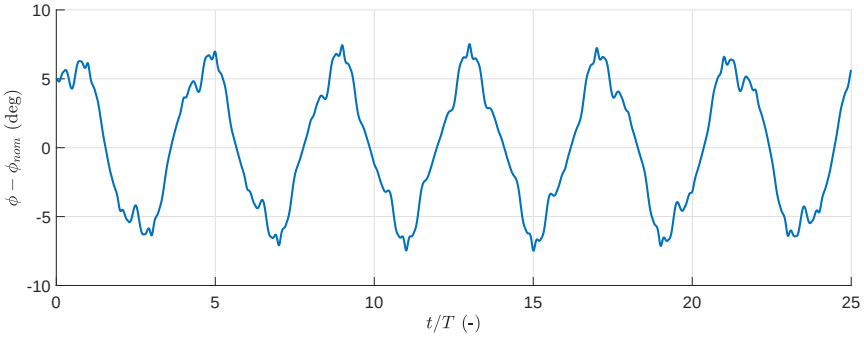


(a) Rotation angle deviation

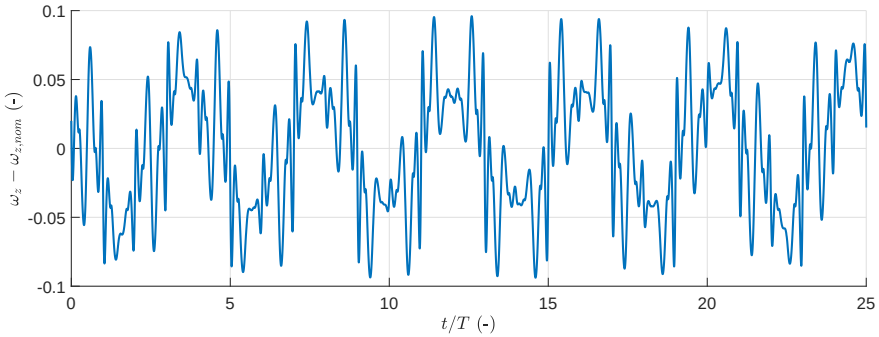


(b) Angular velocity deviation

Figure 16: Perturbed solution profile, deviation from nominal solution. LLS in 1:2 Sun resonant DRO